JOURNAL OF PROPULSION AND POWER
Vol. 11, No. 1, January–February 1995

Microstructural Basis for Enhanced Shock-Induced Chemistry in Single Crystal Ammonium Perchlorate

W. L. Elban*
Loyola College, Baltimore, Maryland 21210
and
H. W. Sandusky,† B. C. Beard,‡ and B. C. Glancy§
Naval Surface Warfare Center, White Oak, Silver Spring, Maryland 20903

The effect of concentrated lattice defects (dislocations) on shock reactivity was investigated for an optical quality, single crystal of high-purity ammonium perchlorate. Prior to shock loading, localized regions of increased lattice defects and strain were created by placing diamond pyramid (Vickers) hardness impressions into exterior cleavage surfaces. The crystal was immersed in mineral oil with the $(\bar{2}\bar{1}0)$ surface 6.0 mm from a detonator. When fired, the detonator delivered a 24.4-kbar shock, corresponding to the reaction threshold for that crystal orientation. High-speed photographs showed luminosity near some of the hardness impressions. The photographs also revealed the occurrence of the same slip deformation identified previously from hardness testing. The shocked crystal was recovered intact and cleaved twice through Vickers impressions on the (001) and shock-entry $(\bar{2}\bar{1}0)$ surfaces, allowing spatial chemical analysis of the interior regions of the crystal using x-ray photoelectron spectroscopy (XPS). Along these freshly cleaved surfaces, the XPS results showed enhanced perchlorate decomposition as a result of the impressions. The greatest decomposition was not immediately adjacent to the impressions, but near the tips of cracks and along slip planes that extended, at least several millimeters, from these impressions.

Introduction

PLASTIC deformation, fracture, and material microstructure have been shown[1] to be important aspects of the shock reactivity of ammonium perchlorate (AP) single crystals. Optically transparent samples (3–10 mm on an edge) were cleaved from aqueous-solution-grown crystals; cleavage planes were parallel to the (001) and $\{\bar{2}10\}$ growth surfaces. Diamond pyramid (Vickers) hardness testing was used[1] to characterize the slip deformation, cracking, and ease of strain energy dissipation on indenting the (001) surface. Many of the same slip and cracking systems observed at low strain rate were active at the high rate experienced during shocking. Prior to shock loading, some crystals had Vickers impressions placed[1] in them to provide localized concentrations of lattice defects (dislocations). The cumulative dislocation strain fields surrounding the impressions should exhibit enhanced chemical reaction.[2,3] Also, the impressions would serve as sites to concentrate additional plastic deformation and cracking during shock loading, possibly contributing to further chemical decomposition.

Crystals were oriented primarily for shock entry normal to the $\{\bar{2}10\}$[1] surface. More recently, limited experiments were conducted with the shock normal to the (001) surface.[4] For both orientations, the respective orthogonal surface was observed with high-speed photography. Shock loading was by a detonator with 0.20 g of explosive at a predetermined stand-off distance in a mineral oil medium. The spherically diverging wave front is conceptually similar to performing a conventional indentation hardness test with a large ball, except that the strain rate for shocking is orders of magnitude greater. A diverging shock, in contrast to a planar shock, permitted the desired activation of slip and cracking systems.

High-speed photographs showed different responses depending on crystal orientation. For shock entry into the $\{\bar{2}10\}$ surface, although not at each shock pressure, the photographs revealed[1] 1) luminosity, presumably associated with chemical reaction, in the vicinity of a (001) surface Vickers impression; 2) a luminous shock front; 3) distinct diagonal lines immediately behind the front that were attributed to the (010)[001] slip system; and 4) a moving luminous band that appeared to be a propagating crack. For shock entry into the (001) surface, the photographs showed[4] no luminosity from either the crystal or microstructural features; however, flame below these crystals was present.

The experimental arrangement permitted soft recovery of many of the crystals. When shocked through the $\{\bar{2}10\}$ surface, recovered crystals were nonuniformly cloudy in appearance and sometimes remained intact, even at shock pressures in excess of the reaction threshold.[1] Crystals that were shocked through the (001) surface exhibited less cloudiness and typically fractured into large pieces.[4] Bulk chemical reaction in large fragments or pieces cleaved from recovered crystals was assessed by liquid ion chromatography (LIC). Based on LIC analysis, the reaction threshold was ~25 kbar for crystals shocked through the $\{\bar{2}10\}$ surface. Only the Cl^- concentration changed significantly relative to an unshocked crystal, whereas there was little consistent change in NO_2^-, NO_3^-, and ClO_3^- levels. In contrast, crystals shocked through the (001) surface had increased concentrations of NO_2^- and NO_3^-, in addition to Cl^-, for shock pressures of 16.7 and 24.4 kbar.

Experimental Approach and Techniques

In the current work, a spatially-specific chemical analysis technique was employed to elucidate further the effect of material microstructure on shock decomposition. A crystal with edge dimensions of approximately 10 × 9 × 7 mm was

Received Aug. 5, 1993; revision received Oct. 26, 1993; accepted for publication April 22, 1994.

*Associate Professor, Department of Electrical Engineering and Engineering Science.
†Research Mechanical Engineer, Detonation Initiation Branch.
‡Research Chemist, Materials Evaluation Branch; currently AKZO-Nobel Chemicals, 1 Livingstone Ave., Dobbferry, NY 10522.
§Research Mechanical Engineer, Explosives Systems Branch.

cleaved from a larger specimen in the same lot used previously.[1] Strain centers were put into both the shock-entry $(\bar{2}10)$ surface and photographically viewed (001) surface by Vickers hardness testing at a load of 9.81 N. The resultant impressions, with diagonal lengths of ~0.5 mm, were of sufficient scale for observing their effect in the shock-loading experiment, designated as Shot ONR-35. To complement the hardness data previously provided[1] for the (001) surface, data for the $\{\bar{2}10\}$ surface of several crystals were obtained for loads ranging from 0.0981 to 9.81 N. The hardness testing procedure is detailed in Ref. 4.

The crystal was then shocked near its reaction threshold. Figure 1 shows the most significant aspects of the setup within the closed chamber, including the field of view of the high-speed camera. For this camera coverage, the framing rate was reduced to 1 million frames/s (vs 2–5 million frames/s previously) to extend the viewing time after shock passage. Also, Kodak TMAX 400 negative film was used to improve resolution relative to previous images[1] on Polaroid® instant print film.

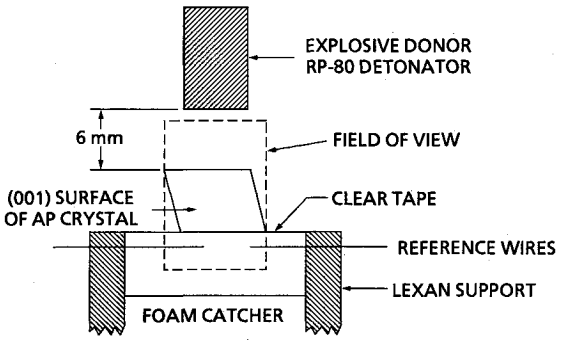

Fig. 1 Arrangement for shock-loading AP crystal immersed in mineral oil showing field of view for framing camera.

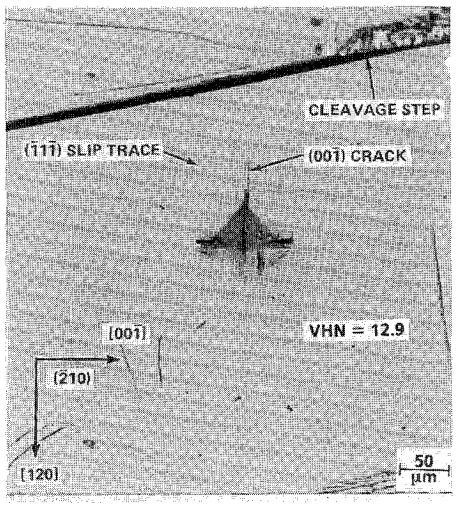

a)

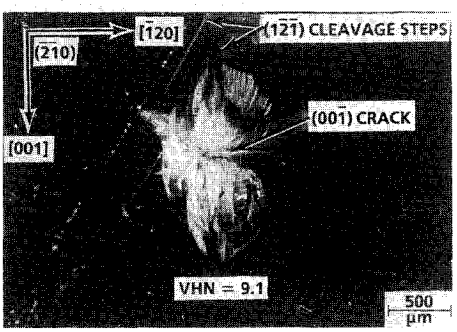

b)

Fig. 2 Diamond pyramid (Vickers) hardness impressions in $\{\bar{2}10\}$ surfaces of AP crystals: a) 0.981-N load on $(\bar{2}10)$ surface and b) 9.81-N load on $(\bar{2}10)$ surface before shock loading, Shot ONR-35.

The crystal was recovered intact and subsequently cleaved through a Vickers impression in each surface, providing two fresh, previously interior $(\bar{2}10)$ planes for analysis. Microstructural analysis was performed on external and freshly cleaved surfaces using light and scanning electron microscopies. XPS was used to scan both cleaved planes. Spectra from the Cl(2p), N(1s), O(1s), and C(1s) photoelectron lines were collected over sampling areas of approximately 1 × 1 mm. This approach allowed the dislocation strain fields associated with the Vickers impressions to be probed to determine quantitatively whether significant chemical decomposition occurred there preferentially. The details of the technique and the correlation of increased Cl(2p) linewidth with dislocation density have been discussed previously for this crystal.[5] The XPS results that follow emphasize the decomposition that was measured. In addition, observations from framing camera photographs of shock interaction with the crystal are related to microstructural features and XPS measurements of decomposition.

Experimental Results

Vickers Hardness Studies

Crystallographic information on slip and cracking systems obtained from Vickers microindentation hardness testing (loads ≤0.981 N) of the (001) and $(\bar{2}10)$ surfaces of AP single crystals has been described in detail previously.[1,6] A transmitted light photomicrograph[6] of an impression put into the $(\bar{2}10)$ surface at 0.981 N load appears in Fig. 2a. Particularly noteworthy is the $(00\bar{1})$ crack that extends from the top corner of the impression. A reflected light photomacrograph of a Vickers impression (9.81 N) that was put into the $(\bar{2}10)$ surface of the crystal used in Shot ONR-35 appears in Fig. 2b. This photomacrograph has been rotated 90 deg, relative to Fig. 2a, to connect directly with the crystal orientation in the shock experiment. The expectation is that the deformation should be the same for indentations put into either surface. However, other deformation systems were activated at higher loads. For the impression in Fig. 2b, a second branch of the $(00\bar{1})$ crack is also present, along with prominent cracking inclined to the $(\bar{2}10)$ surface. The second $(00\bar{1})$ crack branch is obscured by scattered light from the inclined crack planes.

A comparison of Vickers hardness numbers (VHNs), expressed in units of kgf/mm^2, for the impressions in Fig. 2 reveals that a 29.5% decrease in hardness occurred as the load was increased. This trend is consistently maintained for all of the Vickers $\{\bar{2}10\}$ hardness data. The combined results for all of the crystals tested are given in Fig. 3 as a logarithmic plot of force on the indenter vs indentation diagonal and $(00\bar{1})$ crack lengths for forces ranging from 0.0981 to 9.81 N. Two distinct regimes in the data resulted, coinciding with the appearance of the second branch of the $(00\bar{1})$ crack. Below 0.981 N, a slope of 1.91 for the diagonal length data was obtained compared to a value of 2.0 for constant hardness behavior. The emergence of the second $(00\bar{1})$ crack branch above 0.981 N causes a much greater difference, 1.60 vs 2.0. By comparison, the diagonal length data reported[1] for Vickers impressions put into the (001) surface yielded a single straight line with a slope of 1.87. The decrease in hardness for both surfaces is attributed to cracking, which causes a sizeable strain energy release.

Although somewhat scattered, the $(00\bar{1})$ crack length data were fit to two displaced, straight line segments each having a slope of 1.5. A force-crack length dependency having this slope is obtained from indentation fracture mechanics analyses.[7,8] The horizontal displacement in the crack length data is also associated with the appearance of the second branch of the $(00\bar{1})$ crack. Such a shift indicates that the coefficient

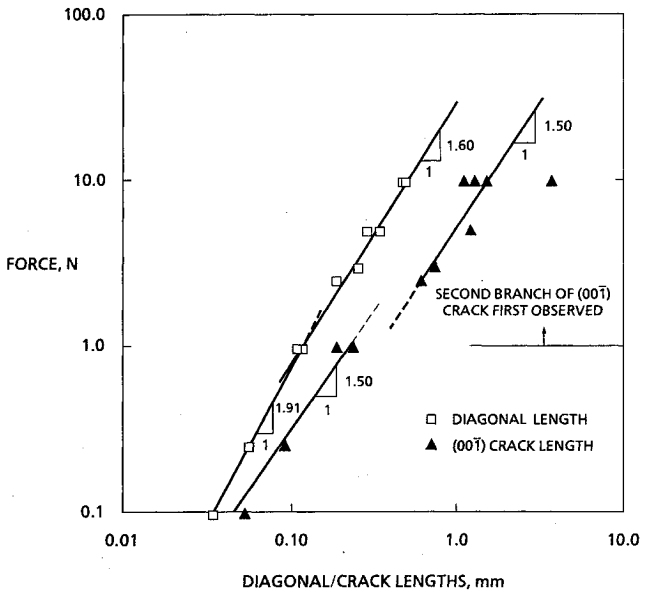

Fig. 3 Force vs diagonal and crack lengths for diamond pyramid (Vickers) impressions in ($\bar{2}$10) or ($\bar{2}\bar{1}$0) surfaces of AP crystals ([00$\bar{1}$] diagonal).

in the fracture mechanics power law dependency (i.e., the indentation fracture mechanics stress intensity[9]) has been diminished by the appearance of the second crack branch. The stress intensity is proportional to $(E\gamma)^{1/2}$, where E is Young's modulus and γ is the fracture surface energy. A dislocation reaction mechanism has been proposed to explain (00$\bar{1}$) crack formation as slip-induced cleavage.[6] As such, it appears that the increased deformation that occurs at higher loads assists the (00$\bar{1}$) cracking.

Shock Loading of Crystal

The damage that results from shock loading the AP crystal to 24.4 kbar in Shot ONR-35 can be seen, relative to the unshocked crystal, in the photomacrographs in Fig. 4. The shocked crystal has nonuniform cloudiness that is most intense at the ($\bar{2}\bar{1}$0) shock-entry surface. The lessening degree of cloudiness from the entry surface correlated at least roughly with shock pressure attenuation. However, the cloudy-clear boundary is not spherical [or circular as viewed through the (001) surface], as might be expected from a spherically diverging shock front. The bottom region of the crystal is still transparent, having the appearance of the unshocked crystal in Fig. 4. Although insufficient to cause cloudiness, some microscopic damage did occur in the bottom region.[5]

High-speed framing photographs from Shot ONR-35 are shown in Fig. 5 for the field of view outlined in Fig. 1. The times associated with each frame are relative to the first frame, which was taken after the shock just entered the crystal at 24.4 kbar. In the first frame (0.0 μs), the shock in the crystal is noticeably curved and has a higher velocity than in the oil. The backlighting continues to be transmitted through the crystal behind the shock, whereas the 15.5-kbar shock in the oil deflects the backlighting. Thus, there is a narrow zone between the two fronts that permits viewing the shocked portion of the crystal. Within that zone, there are dark diagonal lines that are associated with (010)[001] slip. Similar diagonal lines were more clearly shown in Fig. 10 of Ref. 1 for Shot ONR-19, which had a lower shock pressure of 16.7 kbar compared to 24.4 kbar in Shot ONR-35.

In the second frame (1.0 μs), taken just as the shock approaches the bottom of the crystal, there is a relatively wide illuminated zone behind the shock front. This observation is similar to that for Shot ONR-18 (Fig. 9 of Ref. 1), which had the same shock input, but a narrower illuminated zone than

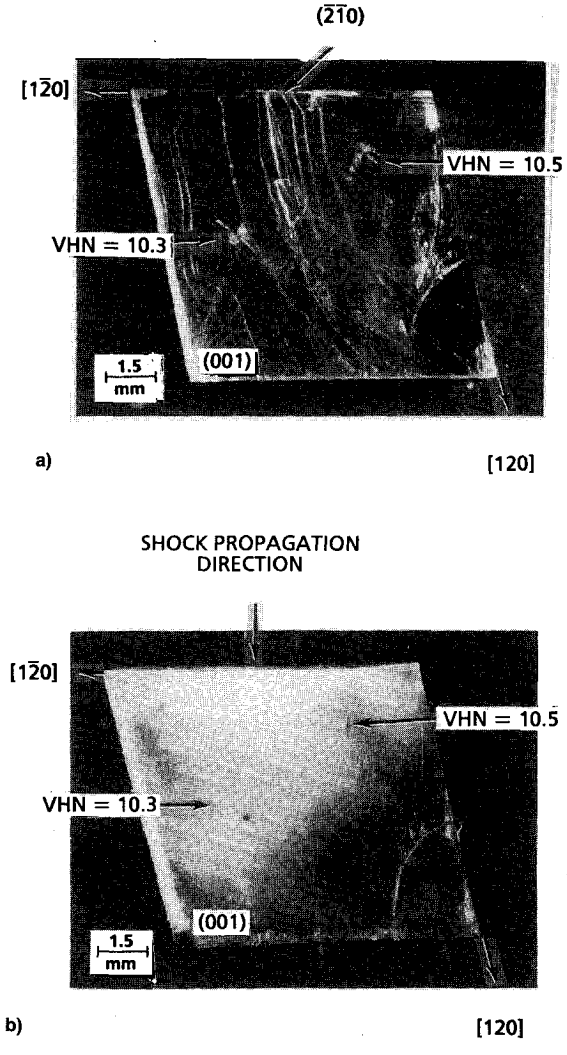

Fig. 4 Photomacrographs of exterior (001) surface of AP crystal a) before and b) after shock entry (to 24.4 kbar) into ($\bar{2}\bar{1}$0) surface.

in Shot ONR-35. Also in Shot ONR-18, the illuminated zone was brighter than the backlighting just below the crystal, indicating light from the chemical reaction of AP. The width of the illuminated zone behind the shock front in ONR-35 may be due partly to reaction light illuminating the crystal behind the shock front, and partly to the increased separation of the shock fronts in the oil and the crystal. As in the previous frame, there are dark diagonal lines just behind the shock front corresponding to (010) slip deformation. One of these lines near the right of the frame is sufficiently broad to suggest that it is associated with a crack. However, the angle of this line relative to the [120] direction is too large to be a ($\bar{1}$21) crack as identified in Fig. 7, which will be discussed later. Further behind the shock front, there are small orthogonal crossing diagonal lines corresponding to both the ($\bar{1}$00) and (010) slip planes, which may not be visible in the photographic reproduction of Fig. 5. The ($\bar{1}$00) lines were not seen in previous dynamic photographs.[1]

By the third frame (2.0 μs), the shock has just exited the bottom of the crystal, which is dark except for a small luminous region near the upper right corner. The size of this region expands in subsequent frames. Pre-existing sources of light in the experiment can be reasonably eliminated as the cause of the luminous region. It is unlikely that hot gaseous detonator products were between the camera and the viewed (001) surface of the crystal, because the luminous region is totally separated from the edge of the crystal in the 2.0- and 3.0-μs frames. It is also improbable that the luminosity was

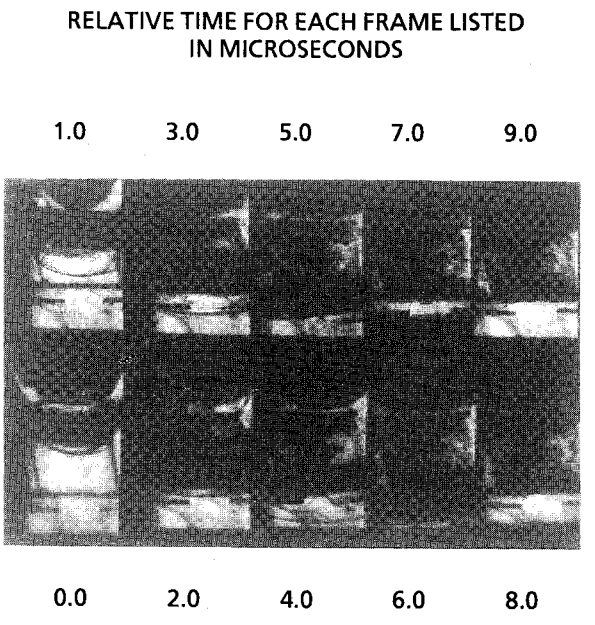

Fig. 5 Backlit framing camera photographs of (001) surface of AP crystal shocked to 24.4 kbar.

transmitted through the crystal, from either backlighting or detonator products. The bottom region of the crystal remained dark after shock passage, even though this region of the recovered crystal was not visibly damaged (Fig. 4b). In contrast, the mineral oil just under the crystal continued to transmit backlighting shortly after shock passage.

A schematic of the crystal, as viewed by the high-speed camera, is given in Fig. 6. The transition from cloudy to clear material and the luminous zone that appeared during shock loading are indicated. The locations of the two cleaved planes, discussed in subsequent sections, are also denoted.

Microstructural Characterization of Recovered Crystal

Referring to the photomicrograph in Fig. 7, numerous ($\bar{1}00$) and (010) slip traces are readily apparent in the as-recovered (001) surface of the center-cleaved section of the Shot ONR-35 crystal. These slip traces are finely spaced, sometimes appearing as shear bands, perhaps indicative of adiabatic heating. The ($\bar{1}00$) traces significantly outnumber the (010) traces, as was observed[1] previously in the recovered AP crystal in Shot ONR-19. In addition to the slip trace formation, numerous ($\bar{1}21$) cracks were found in the Shot ONR-35 crystal that were not observed in the Shot ONR-19 crystal. It is interesting to note that ($1\bar{2}\bar{1}$) cleavage steps were observed (Fig. 2b) in the ($2\bar{1}0$) surface of the AP crystal prior to shock loading in Shot ONR-35. It appears that there is some inherent weakness in the bonding across this plane that explains its propensity for cracking at high stress levels. It is possible that a dislocation reaction occurs, providing the nucleus for crack formation.

Low magnification scanning electron microscope (SEM) photographs of the right-hand cleaved section of the crystal from Shot ONR-35 appear in Fig. 8. The edge region formed by the intersection of the shock-entry ($2\bar{1}0$) surface with cleaved plane no. 1 is shown in Fig. 8a. The major portion of the most prominent ($00\bar{1}$) crack branch that emanated from one corner of the Vickers impression (VHN = 9.1) in the ($2\bar{1}0$) surface is clearly visible. The crack surfaces have separated a distance of ~0.08 mm as a result of the cleaving operation, since virtually no transverse separation in the crack branch was observed in light microscopy photographs of the Vickers impression before or after the crystal was shock loaded. From these photographs, it was determined that the crack branch underwent a radial extension of ≤0.03 mm as a result of shock loading. Also denoted in Fig. 8a is a ($1\bar{2}\bar{1}$) crack, identified by performing a two-trace analysis on optical photographs of the crack intersecting the ($2\bar{1}0$) and (001) surfaces. This observation connects directly with the ($1\bar{2}\bar{1}$) cleavage steps in Fig. 2b and the ($\bar{1}21$) cracks in Fig. 7 discussed earlier.

The portion of cleaved plane no. 1 directly underneath the Vickers impression is shown in Fig. 8b. Considerable surface roughness is present indicating that ($2\bar{1}0$) cleavage cracking did not occur easily. This is attributed to the hindering effect that work hardening, associated with forming the impression and/or shocking the crystal, has on crack propagation. The penetration of the ($00\bar{1}$) crack into the crystal is clearly visible in Fig. 8b. The exact length is obscured by surface roughness ~1.5 mm below the ($2\bar{1}0$) surface. A fine ($00\bar{1}$) crack may actually extend ~2 mm below where the broad separation in the crack terminates (at ~1.25 mm from the shock-entry sur-

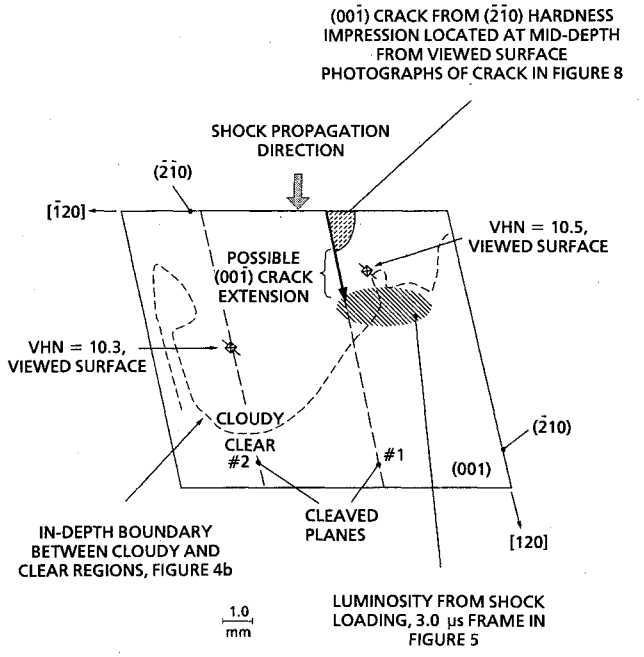

Fig. 6 Schematic of various features viewed on or through (001) surface of the shock loaded/recovered AP crystal.

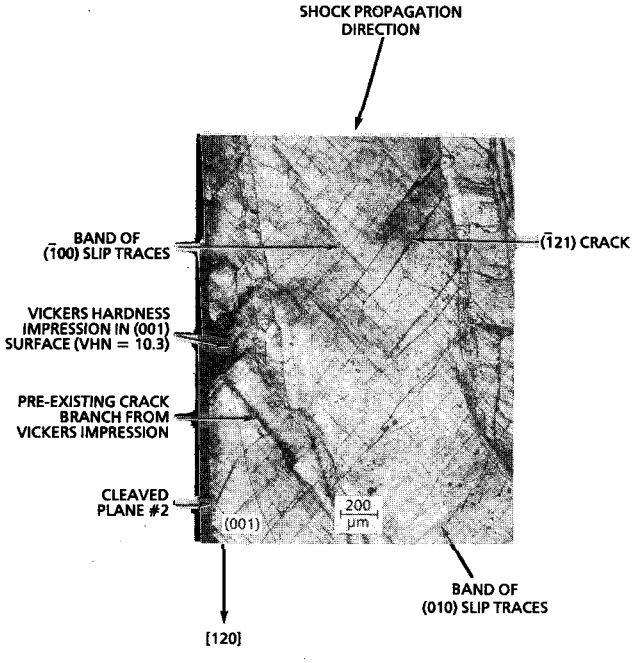

Fig. 7 Reflected light photomicrograph of slip traces and cracking near center of exterior (001) surface of recovered AP crystal.

face). The extent of the broadly separated crack is indicated in Fig. 6, which also shows the possible extension of the fine crack.

XPS Analysis of Recovered Crystal

The results from analysis of the XPS spectra obtained across cleaved plane nos. 1 and 2 are given in Fig. 9. Approximate analysis areas are outlined by the boxes superimposed on schematics of the cleaved planes, including locations of the Vickers impressions. Appearing in the upper half of the boxes are values for %Cl as decomposition products, while spectral linewidth (FWHM) values for the Cl(2p, 3/2) peak are in the bottom half. Comparison with standards indicate that the decomposition product is a Cl(+5) containing compound. The run numbers, providing the order of the analyses, appear at the top of the boxes. Emphasis was given to following the chlorine spectra since the nitrogen spectra showed no indication of chemical change.

Referring to Fig. 9a, spot analyses were performed along the centerline and one edge of cleaved plane no. 1. Spectra were not collected along the opposite edge because of excessive charging. The measured yields of %Cl as decomposition products do not correspond spatially one-to-one with the increased FWHM values. Chemical changes are limited to the centerline area directly underneath the Vickers impression and occur for ~3.5 mm in the [120] direction. This area encompasses the (00$\bar{1}$) crack appearing in Fig. 8b and its strain field. The highest decomposition level [9.5% chlorine in the (+5) state] was found at the termination of the broad separation in the crack. In centerline regions below this, with essentially the same ~1.45 FWHM value, there was no detected chemical decomposition. This was also the case for the corner region near the shock-entry surface having a 1.50 FWHM value.

In Fig. 9b, the spot analyses for cleaved plane no. 2 show that the chemical changes and FWHM values followed a different spatial relationship. In contrast to cleaved plane no. 1, no chemical change was detected in the vicinity of the Vickers impression or immediately below the shock-entry surface. However, there were significant changes measured further below that surface that correspond in location to results obtained for cleaved plane no. 1. Significant chemical changes also occurred toward the bottom along the center and near the edge opposite the indented surface. These changes were in a region where a series of irregular cleavage steps were observed to emanate from the Vickers impression.

Discussion

Time Frame for Crystal Damage and Decomposition

Although the microstructural and chemical analyses were conducted long after shock loading, the high-speed photographs reveal that crystal damage and chemical reaction occurred during the shock process (i.e., loading and subsequent unloading). The cloudy-clear boundary (Fig. 4b) appears in the high-speed photographs (Fig. 5) after the 3.0-μs frame. Thus, the damage observed in the recovered crystal occurred sometime during the shock process rather than from capturing the crystal in foam (Fig. 1).

Chemical reaction is associated with the luminous zone near the upper right corner of the crystal in Fig. 6 since other sources of light in the experiment will not account for the observed light. The luminous zone first appears in the 2.0-μs frame (Fig. 5) just after shock passage. This zone is on the boundary of the in-depth damage, whereas XPS measurements in Fig. 9a place the expected source of luminous reaction (greatest decomposition) closer to the shock-entry surface, in the strain field of the Vickers impression in that surface. The strain field, which is located in the region of the (00$\bar{1}$) crack shown in Fig. 6, resided in the most extensively damaged region of the crystal. Since a direct view of that region was inhibited by the damage, the observed luminosity appears near the in-depth damage boundary. As will be discussed, this boundary deviated toward the shock-entry surface in the region where the luminosity was observed.

Unfortunately, there was not sufficient time resolution in the high-speed photographs to distinguish unequivocally the roles of shock loading and unloading on microstructural changes and consequent enhanced chemical reactivity. The photographs for Shot ONR-19 (Fig. 10 in Ref. 1), in particular, clearly show slip traces joining the shock front, suggesting that the loading process is responsible for the damage observed in recovered crystals (Figs. 11–13 in Ref. 1 and Figs. 4b and 7). However, luminosity attributed to crack propagation (Fig. 9 in Ref. 1), or occurring in the vicinity of the Vickers impressions (Fig. 9 in Ref. 1 and Fig. 5), has always been observed to occur one or more microseconds after shock

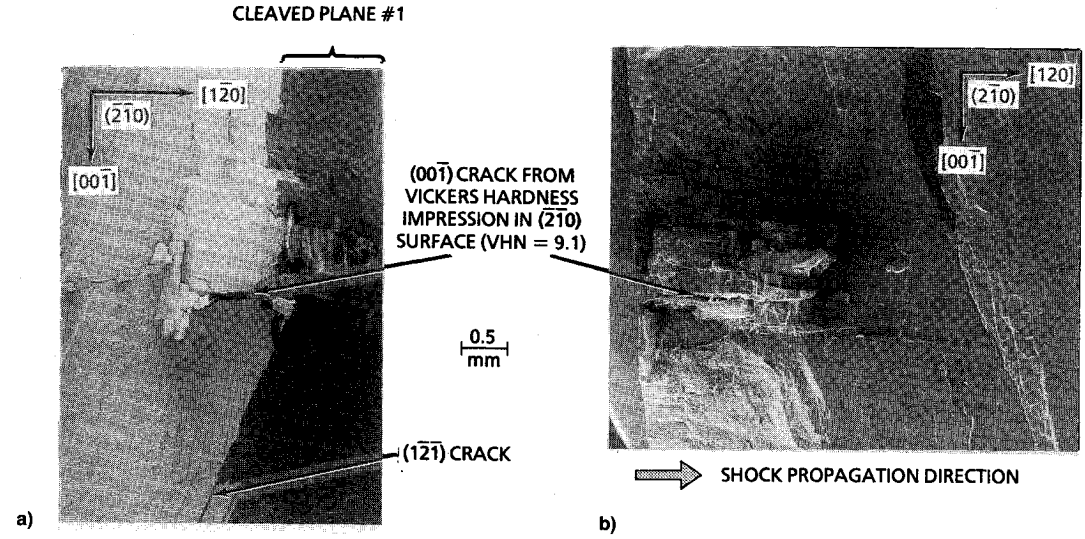

Fig. 8 Low magnification SEM photographs of cracking in vicinity of (2$\bar{1}$0) Vickers hardness impression in recovered AP crystal: a) shock-entry (2$\bar{1}$0) surface and b) cleaved plane no. 1.

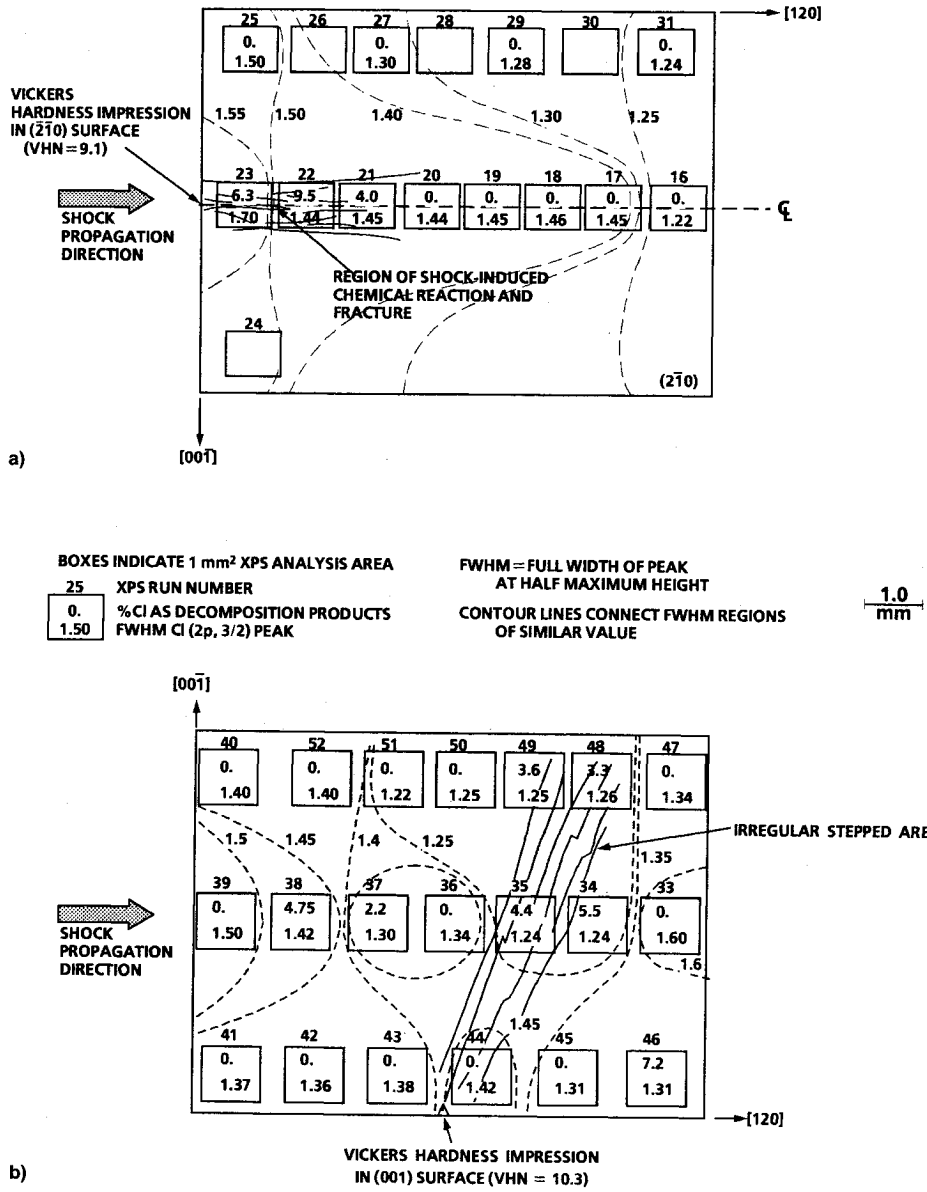

Fig. 9 XPS analysis results from interior of AP crystal shocked to 24.4 kbar. Cleaved plane no. a) 1 and b) 2.

passage. This indicates either that the unloading process influences shock reactivity or that there is an induction time before the onset of reaction.

Decomposition from Shock Loading

The combined XPS results for cleaved planes nos. 1 and 2 indicate that the largest amounts of chemical decomposition were associated with the Vickers impressions put into the crystal prior to shock loading. However from Fig. 9b, the character of the shock (pressure and duration) was sufficient to cause decomposition along the centerline away from the influence of the impression. This provides a confirmation of the previous LIC determination of reaction threshold to be ~24.4 kbar when hardness impressions in the crystal are absent (Shot ONR-17).[1]

Chemical reaction was enhanced in regions where the shock interacted with pre-existing dislocations. The visual damage or change in FWHM values (control crystal[5] having impressions and associated cracking) in these regions prior to shock loading was either not detectable or small compared to the subsequent shock damage. This indicates that the observed chemical effects are shock-driven and cannot be merely attributed to cracking and any accompanying effects. While shock loading enhanced damage in regions with pre-existing dislocations, there were regions unaffected by the Vickers impressions that had similar levels of damage, but greatly reduced extent of reaction. Thus, the extensive damage from shock loading was of much less importance in initiating reaction than the lesser preshock damage.

In the recovered crystal, only the chlorine chemistry was observed to change, with Cl(+7) decomposing to Cl(+5). Production of oxidized nitrogen (i.e., NO, NO_2) or O_2 is likely, but these species are not detectable since the spectrometer used can only analyze solid materials. To explore more fully the solid-state decomposition chemistry of AP, secondary ion mass spectrometry was employed for analyzing products in impacted and irradiated samples. Relative to a control sample from a freshly cleaved single crystal, these damaged samples displayed a mass-to-charge ratio *m/e* peak for Cl(+5), which has been tentatively attributed to $HClO_3$ (*m/e* = 90). Thus, shock passage in the crystal appears to have reduced the perchlorate anion to the chlorate anion as a stable intermediate decomposition product.

Microstructural Response to Shock Loading

The degree of curvature observed for the propagating shock in the 0.0- and 1.0-μs frames in Fig. 5 is less than that for the in-depth boundary of crystal damage appearing in Fig. 4b. The increased curvature for the damage boundary is attributed to lateral rarefactions that reduce the shock intensity and duration. Thus, a threshold condition for shock/rarefaction interplay was present to cause visible damage (cloudiness). The in-depth boundary for crystal damage is uniformly curved except in the vicinity of the two Vickers impressions on the (001) surface. This boundary is extended further from the shock-entry surface for the left impression (VHN = 10.3), whereas cloudiness is greatly reduced in the vicinity of the right impression (VHN = 10.5). The right impression is near the impression in the shock-entry $(2\bar{1}0)$ surface. This suggests that the large $(00\bar{1})$ crack (Fig. 8) associated with the latter impression reduces damage by allowing shock-generated dislocations to escape.

Some of the slip systems involved in accommodating the Vickers indenter at low strain rate were also active in the shocked crystal. In particular, the numerous diagonal lines appearing in some high-speed photographic frames were attributed to two prominent slip systems identified from hardness testing[6]: (010)[001] and (100)[001]. The resultant slip traces were also observed in the external (001) surface of the recovered crystal (Fig. 7). The $(\bar{1}21)$ crack plane, occurring in the shocked crystal, was not involved in forming the indentations and has not been reported previously. The appearance of this crack plane indicates that shocking provided a higher stress normal to this plane than what was present during hardness testing.

Summary and Conclusions

Additional results, to relate to earlier work, have been obtained for the roles that plastic deformation, fracture, and material microstructure have on the shock reactivity of AP. Emphasis was given to a detailed analysis of one experiment in which a large crystal, containing several Vickers hardness impressions, was subjected to a shock at the reaction threshold, ~25 kbar. The crystal was recovered intact. Microstructural characterization was conducted using light and scanning electron microscopies. X-ray photoelectron spectroscopy was used to scan 1- × 1-mm areas across two freshly cleaved surfaces that cut right through the Vickers impressions. The most significant finding was that the largest amounts of chemical decomposition occurred because of the presence of the impressions. For the impression put into the shock-entry $(2\bar{1}0)$ surface, decomposition was detected directly underneath over a depth of 3.5 mm and seemed to be associated with a large $(00\bar{1})$ crack that formed at the impression prior to shock loading and possibly had penetrated to that distance. For an impression put into the (001) surface, no evidence of decomposition was found in close proximity. Rather, decomposition was detected in an area of irregular cleavage steps that emanated from the impression and extended the entire depth of the crystal, ~7 mm. A series of high-speed photographs taken during shock loading of the crystal revealed an enlarging, elliptically-shaped luminous zone located off center from, but encompassing, the furthest possible extension of the $(00\bar{1})$ crack. The combined observations indicate that the luminosity resulted from chemical reaction occurring either at the tip of the $(00\bar{1})$ crack or in its plastic zone.

Acknowledgments

This work was supported by the Office of Naval Research under work request numbers N00014-87-K-0175 and N00014-85-WR-24103 as a cooperative effort between Loyola College, Baltimore, and the Naval Surface Warfare Center (NAVSWC), White Oak Detachment. Support was also provided by the Independent Research Program at NAVSWC. Richard R. Bernecker, NAVSWC, and Sigmund J. Jacobs, Advanced Technology and Research, Inc., provided many helpful comments and guidance concerning the early direction of the work. R. R. Bernecker also provided an extensive review of the current paper. Numerous helpful discussions were held with Ronald W. Armstrong, Department of Mechanical Engineering, University of Maryland, College Park (UMCP), concerning the hardness testing, SEM, and XPS results. Large (>1 cm), optical quality, pure single crystals of AP were provided by Thom L. Boggs, Naval Air Warfare Center, China Lake, California. Dorn W. Carlson and Sybil S. Turner, NAVSWC, performed the LIC analysis on recovered crystals. Marriner K. Norr, NAVSWC, obtained the low magnification SEM photographs in Fig. 8. Donald A. Keefer, Department of Biology, Loyola College, helped with the transmission light microscopy used to obtain Fig. 2a. Xian Jie Zhang, UMCP, printed the photograph appearing in Fig. 2a.

References

[1]Sandusky, H. W., Glancy, B. C., Carlson, D. W., Elban, W. L., and Armstrong, R. W., "Relating Deformation to Hot Spots in Shock-Loaded Crystals of Ammonium Perchlorate," *Journal of Propulsion and Power*, Vol. 7, No. 4, 1991, pp. 518–525.

[2]Thomas, J. M., "Enhanced Reactivity at Dislocations in Solids," *Advances in Catalysis and Related Subjects*, Academic Press, New York and London, 1969, pp. 293–400.

[3]Thomas, J. M., "The Chemistry of Deformed and Imperfect Crystals," *Endeavour*, Vol. 29, No. 108, 1970, pp. 149–155.

[4]Elban, W. L., Sandusky, H. W., Beard, B. C., and Glancy,

B. C., "Investigation of the Origin of Hot Spots in Deformed Crystals: Final Report on Ammonium Perchlorate Studies," Naval Surface Warfare Center, NSWCDD/TR-92/206, Silver Spring, MD, July 1993.

[5]Beard, B. C., Sandusky, H. W., Glancy, B. C., and Elban, W. L., "Defect Density Measurements in Shocked Single Crystal Ammonium Perchlorate by X-Ray Photoelectron Spectroscopy," *Journal of Materials Research*, Vol. 7, No. 12, 1992, pp. 3266–3274.

[6]Elban, W. L., Coyne, P. J., Jr., Sandusky, H. W., Glancy, B. C., Carlson, D. W., and Armstrong, R. W., "Investigation of the Origin of Hot Spots in Deformed Crystals: Studies on Ammonium Perchlorate and Reference Inert Materials," Naval Surface Warfare Center, NSWC MP 88-178, Silver Spring, MD, April 1988.

[7]Frank, F. C., and Lawn, B. R., "On the Theory of Hertzian Fracture," *Proceedings of the Royal Society of London, Series A*, Vol. 299, No. 1458, 1967, pp. 291–306.

[8]Lawn, B. R., and Fuller, E. R., "Equilibrium Penny-Like Cracks in Indentation Fracture," *Journal of Materials Science*, Vol. 10, No. 12, 1975, pp. 2016–2024.

[9]Armstrong, R. W., and Elban, W. L., "Cracking at Hardness Micro-Indentations in RDX Explosive and MgO Single Crystals," *Materials Science and Engineering*, Vol. A111, 1989, pp. 35–43.